Polarization Properties of a Single-Mode Operating Gas Laser in a Small Axial Magnetic Field

W. Van Haeringen

Philips Research Laboratories, N. V. Philips' Gloeilampenfabrieken, Eindhoven, The Netherlands

(Received 3 January 1967)

The polarization properties of a single-mode operating gas laser in a small axial magnetic field (field splitting≪natural linewidth) with an initial cavity anisotropy are considered in detail. Expressions are given for the effects on the polarization parameters due to the active medium, the external field, and the initial anisotropy of the cavity. The cooperation of these three effects is discussed. Existing theories are in this respect shown to be either incomplete or inadequate. Specializations are made to several types of atomic transitions and cavity anisotropies. A group of low-field polarization phenomena observed on the He–Ne 1.153-μ mode is theoretically discussed. In particular, it is shown that the observed polarization flip by tuning through the line center and the hysteresis effect, observed by Kannelaud and Culshaw, can be completely understood assuming a cavity whose main anisotropy is a linear phase anisotropy. At zero or very small magnetic field the theory predicts a preference for linear or circular polarization, depending on the type of atomic transition.

I. INTRODUCTION

A GAS laser shows in general a variety of polarization phenomena, which have been the subject of both experimental and theoretical studies.

An important group of experiments concern the behavior of the He–Ne 1.153-μ mode not too close to threshold. The mode then shows linear polarization. Rotations of the polarization plane in axial fields of a few Oe were reported by Statz, Paananen, and Koster,[1] Culshaw and Kannelaud,[2] and De Lang and Bouwhuis.[3] No steady rotation was observed for fields smaller than some critical $H_{crit.}$ (about 1 Oe or less). In the latter case, the stable polarization azimuth ϑ was observed to depend on the external field.[2,3] When H was varied from 0 to $\pm H_{crit.}$, the stable polarization plane was observed to rotate through an angle of $\pm\frac{1}{4}\pi$. Furthermore, at $H=0$ the stable polarization plane flipped into a position differing by about an angle $\frac{1}{2}\pi$ when the laser was tuned through the center of the Doppler profile. This polarization flip does not occur abruptly at line center[4]; it is furthermore accompanied by a hysteresis effect. The latter effect, first observed by Kannelaud and Culshaw,[4] implies that, in the direct neighborhood of the line center, the polarization plane chooses its position according to the tuning history of the laser.

In the interpretation of the above experimental facts, the first question to be answered is why the He–Ne 1.153-μ mode shows the observed preference for linear polarization at all. Induced by experiments of De Lang, Bouwhuis, and Ferguson,[5] who were able to measure the "strength" of this linear preference, this

question was solved by Polder and Van Haeringen[6] by applying Lamb's theory[7] to the case of degenerate atomic levels ($H=0$). Depending on the type of atomic transition, their theory predicted the kind and size of the polarization preference. In the above case of a He–Ne 1.153-μ mode (a $j=1\rightarrow j=2$ transition) there was full agreement with the experiments of De Lang et al,[5] whereas later experiments[8] gave examples of He–Ne modes showing circular preference. For instance, the He–Ne 1.207-μ mode (a $j=2\rightarrow j=2$ transition) shows circular preference,[8] in agreement with the theory. In this connection we should like to mention the work of Heer and Graft[9] and Doyle and White,[10] who made similar extensions of Lamb's theory, without, however, giving the explicit medium-induced nonlinear effects on the polarization ellipse for all types of atomic transitions.

The observed stability of the polarization plane (He–Ne 1.153-μ mode) for external fields running from zero to some critical value and the (nonuniform) rotation of the polarization plane for fields surpassing this critical value cannot be understood without the assumption of a cavity with an initial anisotropy. This view is commonly accepted.[3,4,10,11] The type of anisotropy assumed by Kannelaud and Culshaw[4] and D'Yakonov[11] is a linear absorption anisotropy, which indeed explains a number of polarization phenomena at low fields. According to De Lang and Bouwhuis,[3] however, such an absorption anisotropy cannot explain the polarization flip mentioned above. According to them the most important anisotropy of the cavity is a linear phase anisotropy, as the observed flip is of a

[1] H. Statz, R. Paananen, and G. F. Koster, J. Appl. Phys. **33**, 2319 (1962).
[2] W. Culshaw and J. Kannelaud, Phys. Rev. **136**, 1209 (1964).
[3] H. de Lang and G. Bouwhuis, Phys. Letters **19**, 481 (1965).
[4] J. Kannelaud and W. Culshaw, Phys. Rev. **141**, 237 (1966).
[5] H. de Lang, G. Bouwhuis, and E. T. Ferguson, Phys. Letters **19**, 482 (1965).

[6] D. Polder and W. van Haeringen, Phys. Letters **19**, 380 (1965).
[7] W. E. Lamb, Jr., Phys. Rev. **134**, A1429 (1964).
[8] H. de Lang and G. Bouwhuis, Phys. Letters **20**, 383 (1966).
[9] C. V. Heer and R. D. Graft, Phys. Rev. **140**, A1088 (1965).
[10] W. M. Doye and M. B. White, Phys. Rev. **147**, 359 (1966).
[11] M. I. D'Yakonov, Zh. Eksperim. i Teor. Fiz. **49**, 1169 (1965) [English transl.: Soviet Phys.—JETP **22**, 812 (1966)].

dispersive nature. Furthermore, a theory in which a linear phase anisotropy is assumed neatly accounts for the reported hysteresis phenomenon,[4] as is shown in the present article.

In our opinion the existing theories of mode polarization in anisotropic cavities with or without small external magnetic fields are incomplete. The theory of De Lang and Bouwhuis,[5,8,12] which does, indeed, account for all of the above-mentioned phenomena, is a phenomenological one and needs a microscopic justification. The theory of Culshaw and Kannelaud[13] assumes absorptive anisotropies only and is restricted to $j = \frac{1}{2} \rightarrow j = \frac{1}{2}$ transitions. Heer and Graft[9] treat the polarization problem for isotropic cavities only. The theory of Doyle and White[10,14] is claimed to be valid for very small excitation densities only. In the theory of D'Yakonov, the possibility of circular polarization preference at zero magnetic field seems to have been overlooked. Moreover, only cavities with a linear absorption anisotropy are considered. The treatment of the external magnetic field in this theory is, however, rather general (field splitting $\ll$ Doppler linewidth).

The present article deals with the single-mode behavior of a gas laser, taking into account the effects of small axial magnetic fields (field splitting $\ll$ natural linewidth), of nonlinearities induced by the active medium, and of the anisotropic cavity (anisotropies of any kind). All types of atomic transitions are considered. Expressions are given for the medium-, the cavity-, and the magnetic-field-induced effects on the polarization parameters. In principle, the theory can be extended to higher field regions and multimode operation. Our main application will be the above-mentioned polarization phenomena.

In the derivation of the equations of motion for the polarization ellipse, we assume the presence of a nearly monochromatic electric field. It has to obey Maxwell's equations, with an anisotropic loss tensor, accounting for both isotropic and anisotropic losses. Before the induced polarization vector $\mathbf{P}$ (to the third order in the electric field $\mathbf{E}$ and to the first order in an external magnetic field $\mathbf{H}$) is calculated, it appears to be very practical (Sec. II) to give a phenomenological equation for the $\mathbf{P}$ vector first, in terms of the $\mathbf{E}$ and $\mathbf{H}$ vectors. It can easily be derived from symmetry properties that the quantum-mechanical calculation of $\mathbf{P}$ can be concentrated on the calculation of six (complex) phenomenological constants. For convenience Maxwell's equations for the electric field (having right- and left-circular amplitudes and phases $E\pm$ and $\phi\pm$) are transformed from the beginning into equations for the ellipticity, the phase difference, the intensity, and the total phase. As the total phase is an insignificant quantity, we end Sec. II with three phenomenological equations of

motion for the ellipticity, the polarization azimuth, and the intensity. The effects of the active medium, the magnetic field, and the empty cavity are clearly separated. Section III and Appendices A and B give calculations of the six phenomenological constants, in which Lamb's theory is applied to the case of degenerate atomic levels.[6,7] In the third-order calculation of $\mathbf{P}$ we do not limit ourselves to the Doppler limit, as in Lamb's work. As a result, we find an additional dispersive nonlinear term proportional to the local derivative in the velocity distribution of the atoms, which becomes relevant for operation not too close to the line center. At the end of Sec. III, the expression for $\mathbf{P}$ is specialized to the case of equal Landé factors for the upper and lower levels. In Sec. IV the equations from Sec. II, in which the phenomenological constants are now known from the calculation in Sec. III, are applied to the following cases: (a) Zero magnetic field and isotropic cavity; (b) Zero magnetic field and anisotropic cavity; (c) Small magnetic field and anisotropic cavity. In case (a) the pure medium-induced equations of motion are obtained. Three classes of atomic transitions are found, the first class having a preference for linear polarization, the second class leading to circular bistability, and the third class leading to no preference at all. Only the predictions concerning the latter class ($0 \leftrightarrow 1$ and $1 \rightarrow 1$ transitions) seem to be in disagreement with experiments.[8,15] Representatives of this class show a slight circular preference. We conclude that a subtle prediction of precise balance (no polarization preference) cannot be taken seriously in our approximate theory.

In cases (b) and (c) the discussion is concentrated on the atomic transition class with linear preference, as the He–Ne 1.153-μ mode will be our main application. In Sec. V we deal more specifically with an isotropic cavity, a cavity with linear absorption anisotropy, a cavity with linear phase anisotropy, and a cavity with combined linear absorption and phase anisotropy. It is shown that a linear phase anisotropy in combination with a relatively very small linear absorption anisotropy has to be adopted in the description of the polarization phenomena mentioned above. The theory gives a satisfactory explanation for all low-field phenomena, including the polarization flip and the hysteresis effect. Finally, we note that the predictions concerning the cavity anisotropies can be checked experimentally by adding anisotropic elements to the cavity.[3,12]

II. ELECTROMAGNETIC FIELD EQUATIONS

In accordance with Lamb,[7] the electric field within the medium is assumed to obey the equation

$$\text{curl curl} \mathbf{E}(z, t) + \mu_0 \mathbf{\Gamma} \cdot (\partial/\partial t) \mathbf{E}(z, t)$$
$$+ \mu_0 \epsilon_0 (\partial^2/\partial t^2) \mathbf{E}(z, t) = -\mu_0 (\partial^2/\partial t^2) \mathbf{P}(z, t). \quad (1)$$

[12] H. de Lang, Physica **33**, 163 (1967).
[13] W. Culshaw and J. Kannelaud, Phys. Rev. **141**, 228 (1966).
[14] W. M. Doyle and M. B. White, Phys. Rev. Letters **17**, 467 (1966).

[15] R. L. Fork, W. J. Tomlinson, and L. J. Heilos, Appl. Phys. Letters **8**, 162 (1966).

The isotropic cavity loss, as well as all initial cavity anisotropies (i.e., without the anisotropies induced by the active medium and external field) are described by the Γ tensor. It is assumed that all these cavity properties may be treated in a "smeared out" way, i.e., continuously in time.

The effect of the active atoms is contained in the macroscopic polarization vector $\mathbf{P}(z, t)$, where z is the coordinate along the axis of the interferometer. The vector $\mathbf{P}$ will depend on the electric field $\mathbf{E}$, on external magnetic fields $\mathbf{H}$, on the pump strength, and on the characteristics of the atomic transitions. In Sec. III, expressions are derived for $\mathbf{P}$ to the third order in $\mathbf{E}$ and to the first order in an axial magnetic field $\mathbf{H}$ for different types of atomic transitions. This will be sufficient for fields E and H which are not excessively large.

It is our task to study the cooperative effect on the electric field in the cavity of the active medium on the one hand and the (anisotropic) cavity on the other hand.

We are confining ourselves to the case of one-mode operation. The electric field satisfying (1) is supposed to be given by

$$\mathbf{E}(z, t) = \tfrac{1}{2} (E_+(t) (\mathbf{x}-i\mathbf{y}) \exp\{-i[\nu t+\phi_+(t)]\} + E_-(t) (\mathbf{x}+i\mathbf{y}) \exp\{-i[\nu t+\phi_-(t)]\}) \sin Kz + \text{c.c.,} \qquad (2)$$

where the right- and left-circular amplitudes and phases E_+, E_- and ϕ_+, ϕ_-, respectively, vary slowly in time; ν is the circular frequency of operation; $K=2\pi n/L$, where L is twice the distance between the mirrors; $\mathbf{x}$ and $\mathbf{y}$ are unit vectors. Once the $\mathbf{P}$ vector has been calculated [by a treatment of the dipole transitions induced by the electric field (2)], the time evolution of the $\mathbf{E}$ field can be found from (1).

Equation (1) is dealt with, by making the same approximations as Lamb,[7] i.e., assuming $\partial^2\mathbf{P}/\partial t^2 = -\nu^2\mathbf{P}$, neglecting second time derivatives and products of first derivatives of E_+, E_-, ϕ_+, and ϕ_- and using $\mu_0\Gamma \cdot \partial\mathbf{E}/\partial t = -i\mu_0\Gamma \cdot \nu\mathbf{E}$.

In accordance with these approximations, we can write the $\mathbf{P}$ vector in the following form:

$$\mathbf{P}(z, t) = \tfrac{1}{2} ([P_+(t)+iQ_+(t)](\mathbf{x}-i\mathbf{y}) \exp\{-i[\nu t+\phi_+(t)]\}$$

$$+ [P_-(t)+iQ_-(t)](\mathbf{x}+i\mathbf{y}) \exp\{-i[\nu t+\phi_-(t)]\}) \sin Kz + \text{c.c.,} \qquad (3)$$

where the real functions P_+, P_-, Q_+, and Q_- vary slowly in time. The explicit form of these four functions follows from the quantum-mechanical treatment in Sec. III. The Q_+, Q_- functions describe the absorptive properties of the medium; the P_+, P_- functions describe the dispersive properties.

Before calculating, however, the $P_\pm$ and $Q_\pm$ functions, we can give phenomenological expressions for them for considerations of symmetry. This runs as follows:

In an isotropic medium with an external dc magnetic field $\mathbf{H}$ and an electric field of the form [see (2)]

$$\mathbf{E} = \mathcal{E} \exp(-i\nu t) + \mathcal{E}^* \exp(+i\nu t), \qquad (4)$$

it is easy to find a formal expression for the polarization vector at frequency ν [see (3)] in terms of $\mathbf{E}$ and $\mathbf{H}$. Let

$$\mathbf{P} = \mathfrak{P} \exp(-i\nu t) + \mathfrak{P}^* \exp(+i\nu t). \qquad (5)$$

We then find

$$\mathfrak{P} = s_1\mathcal{E} + s_2(\mathcal{E} \times \mathbf{H}) + s_3(\mathcal{E} \cdot \mathcal{E}^*)\mathcal{E} + s_4(\mathcal{E} \cdot \mathcal{E})\mathcal{E}^* + s_5(\mathcal{E} \cdot \mathcal{E}^*)(\mathcal{E} \times \mathbf{H}) + s_6(\mathcal{E} \cdot \mathcal{E})(\mathcal{E}^* \times \mathbf{H}) + s_7(\mathcal{E} \times \mathcal{E}^*)(\mathcal{E} \cdot \mathbf{H}) + \cdots. \qquad (6)$$

In (6) we limit ourselves, as announced above, to the third order in $\mathcal{E}$ and the first order in $\mathbf{H}$. The seven constants s_1 to s_7 are generally complex. The $\mathbf{E}$ and $\mathbf{P}$ field in (2) and (3) are perpendicular to the z axis. This implies that the s_2, s_5, and s_6 terms in (6) contribute only when $\mathbf{H}$ has an axial component. The s_7 term in (6) drops out if we specialize to the case of axial magnetic fields. Substitution of (2) and (3) in (6) directly provides the desired phenomenological expressions for the absorptive $Q_\pm(t)$ functions and the dispersive $P_\pm(t)$ functions. Specializing to axial magnetic fields H_z we find

$$(\nu/\epsilon_0)Q_\pm = -\alpha E_\pm \pm \alpha' E_\pm H_z + \beta_1 E_\pm^3 + \beta_2 E_\pm E_\mp^2 \pm \beta'_1 E_\pm^3 H_z \pm \beta'_2 E_\pm E_\mp^2 H_z, \qquad (7)$$

$$(\nu/\epsilon_0)P_\pm = -\sigma E_\pm \pm \sigma' E_\pm H_z + \rho_1 E_\pm^3 + \rho_2 E_\pm E_\mp^2 \pm \rho'_1 E_\pm^3 H_z \pm \rho'_2 E_\pm E_\mp^2 H_z, \qquad (8)$$

where the twelve coefficients α, α', σ, σ', β_1, β'_1, β_2, β'_2, ρ_1, ρ'_1, ρ_2, and ρ'_2 are real. The factor ν/ϵ_0 in front of $Q_\pm$ and $P_\pm$ is written for (later) convenience.

Writing the loss tensor

$$\Gamma = \epsilon_0 \begin{pmatrix} \Gamma_{++} & \Gamma_{+-} \\ \Gamma_{-+} & \Gamma_{--} \end{pmatrix} \qquad (9)$$

as the sum of an isotropic loss, a linear absorption and phase anisotropy (different main axes in general), and a circular absorption and phase anisotropy (see Appendix A), we can easily rewrite Eq. (1) by substituting (2), (3), (7), and (8) in a set of four differential equations for the amplitudes $E_\pm$ and the phases $\phi_\pm$. It is, however, practical to introduce the quantities

$$\chi(t) = \arctan(E_- - E_+)/(E_- + E_+), \tag{10}$$

$$\vartheta(t) = \tfrac{1}{2}(\phi_- - \phi_+), \tag{11}$$

$$I(t) = E_-^2 + E_+^2, \tag{12}$$

where χ is the angle indicating the ellipticity of the mode $(-\tfrac{1}{4}\pi \leq \chi \leq +\tfrac{1}{4}\pi)$, ϑ is the angle made by the long axis of the polarization ellipse with a fixed axis $(0 \leq \vartheta < \pi)$, and I is the intensity of the mode. A fourth independent quantity is $\tfrac{1}{2}(\phi_- + \phi_+)$, in which we are not interested.

Rewriting (1) in terms of χ, ϑ, and I gives the following equivalent set of coupled equations:

$$d\chi/dt = \tfrac{1}{8}(\beta_2 - \beta_1)I\,\sin4\chi + \tfrac{1}{2}H_z[\alpha' + \tfrac{1}{2}(\beta'_1 + \beta'_2)I]\,\cos2\chi + h_1(\chi, \vartheta), \tag{13}$$

$$\cos2\chi(d\vartheta/dt) = \tfrac{1}{8}(\rho_2 - \rho_1)I\,\sin4\chi + \tfrac{1}{2}H_z[\sigma' + \tfrac{1}{2}(\rho'_1 + \rho'_2)I]\,\cos2\chi + h_2(\chi, \vartheta), \tag{14}$$

$$I^{-1}(dI/dt) = \alpha - \tfrac{1}{2}(\beta_1 I)(1 + \sin^2 2\chi) - \tfrac{1}{2}(\beta_2 I)\cos^2 2\chi + H_z(\alpha' + \beta'_1 I)\sin2\chi - \mathrm{Re}\Gamma + h_3(\chi, \vartheta), \tag{15}$$

where the effect of the anisotropic cavity (Appendix A) shows up in the h_1, h_2, and h_3 terms

$$h_1(\chi, \vartheta) = \tfrac{1}{2}a\,\cos2(\vartheta - \vartheta_1)\,\sin2\chi + \tfrac{1}{2}\phi_0\,\sin2(\vartheta - \vartheta_2) + \tfrac{1}{2}a', \tag{16}$$

$$h_2(\chi, \vartheta) = \tfrac{1}{2}a\,\sin2(\vartheta - \vartheta_1) - \tfrac{1}{2}\phi_0\,\cos2(\vartheta - \vartheta_2)\,\sin2\chi - \tfrac{1}{2}\phi', \tag{17}$$

$$h_3(\chi, \vartheta) = -a\,\cos2(\vartheta - \vartheta_1)\,\cos2\chi + a'\,\sin2\chi. \tag{18}$$

The meaning of Γ, a, ϕ_0, a', ϕ', ϑ_1, and ϑ_2 is given in Appendix A. Equations (13)–(15) are our basic equations. There is a clear distinction in the right-hand sides of (13)–(15) between the effects due to the medium and those due to the empty cavity.

An inspection of (13)–(15) already shows something of the physical significance of the respective terms. Let us first discuss the effects of the medium. Suppose we start at $t = t_0$ with a field characterized by $I(t_0)$, $\chi(t_0)$, and $\vartheta(t_0)$. As I and χ are functions of $E_\pm$ only, the initial behavior of $I(t)$ and $\chi(t)$ will be completely determined by the absorptive part of the **P** vector. This manifests itself in (13) and (15) where we meet only coefficients from the expansion of the absorptive $Q_\pm$ functions (i.e., α, α', β_1, β_2, β'_1, and β'_2). On the other hand, $\vartheta(t)$, being half the phase difference of the left and right circularly polarized parts of the wave, is, in its initial behavior, determined by the dispersive part of the **P** vector. Therefore, (14) contains only coefficients of the dispersive $P_\pm$ functions (i.e., σ', ρ_1, ρ_2, ρ'_1, and ρ'_2).

Consider the case where left and right circular parts of the wave are uncoupled $[\beta_2 = \rho_2 = \beta'_2 = \rho'_2 = 0$, see Eqs. (7) and (8)$]$, and take $H_z = 0$. If there is an initial difference in E_+ and E_-, i.e., if initially $\chi(t_0) \neq 0$, both the ellipticity $\chi(t)$ and the phase difference $\vartheta(t)$ change [owing to the first terms in (13) and (14)]. This is a well-known saturation phenomenon: Because of nonlinear effects, the less saturated part of the mode can grow more rapidly than the more saturated part. If there is a nonvanishing coupling between the two parts of the mode $(\beta_2, \rho_2, \beta'_2, \rho'_2 \neq 0)$, the former effect

is slightly altered because of additional conversion of left- and right-polarized parts into each other. In this way the origin of the terms in (13) and (14) proportional to $\sin4\chi$ can be understood. This saturation effect also shows up in Eq. (15) in the terms proportional to β_1 and β_2.

An axial magnetic field gives rise in general to a rotation of the polarization ellipse. The magnetic field induces a dispersive anisotropy [see Eq. (14)] and an absorptive anisotropy [see Eqs. (13) and (15)]. The magnetic-field term in (15) will be negligible in the cases to be considered (Zeeman splitting $\ll$ natural linewidth).

The effect of the empty cavity on the behavior of χ, ϑ, and I is complicated in the case of a general Γ tensor. However, writing the Γ tensor as a sum of an isotropic part and a finite number of known anisotropies [Appendix A] is very helpful; we can easily specialize the cavity terms (16), (17), and (18) to cases of interest in which one or more of the anisotropies a, ϕ_0, a', ϕ' are zero. For an isotropic cavity, the only remaining cavity term is the isotropic loss $- \mathrm{Re}\Gamma$ appearing in Eq. (15).

III. QUANTUM-MECHANICAL TREATMENT OF THE POLARIZATION

The active medium is assumed to consist of atoms each of which has two relevant energy levels a and b. These levels are degenerate and are characterized by angular-momentum quantum numbers j_a and j_b. In an external magnetic field **H**, they split up into $2j_a + 1$

sublevels with energy

$$\hbar\omega_{a_m} = \hbar\omega_a + mg_a\mu_B \,|\,\mathbf{H}\,| \qquad (19)$$

and $2j_b+1$ sublevels with energy

$$\hbar\omega_{b_m} = \hbar\omega_b + mg_b\mu_B \,|\,\mathbf{H}\,|, \qquad (20)$$

where m is the magnetic quantum number running from $-j_a$ to $+j_a$ or $-j_b$ to $+j_b$, g_a (g_b) is the Landé factor for the upper (lower) level, and μ_B is the Bohr magneton.

If an atom at z_0 with axial velocity v_z is excited in one of the above states at t_0, the atom can make transitions owing to a disturbance of the electric-dipole type

$$\mathcal{K}' = -e\mathbf{r}\cdot\mathbf{E}[z_0+v_z(t-t_0),\,t], \qquad (21)$$

where $\mathbf{E}$ is given by (2), and where e and $\mathbf{r}$ are the electron charge and coordinate. Let the undisturbed eigenstates be ψ_{a_m} and ψ_{b_m}, respectively; we then define

$$\int \psi_{a_m}{}^{*}\mathcal{K}'\psi_{b_{m+h}}d\tau \equiv \hbar V_t(a_m,\,b_{m+h}), \qquad (22)$$

where, because of the selection rules, h can be -1, 0, or $+1$. As we are specializing in axial magnetic fields, the $h=0$ case is absent if we choose the quantization

axis to be the z axis. We further need the quantities

$$e\int \psi_{a_m}{}^{*}(x\pm iy)\psi_{b_{m\mp1}}d\tau = p_{m,m\mp1}. \qquad (23)$$

Let the spontaneous (density) decay times for each of the upper and lower levels be γ_a^{-1} and γ_b^{-1}, respectively; let $\gamma_{ab}=(\gamma_a+\gamma_b)/2$ and let the number of atoms excited per unit volume and time in sublevel α, by means of an external pump, Λ_α, be independent of place and time. This Λ_α is distributed over the respective atomic velocity groups by the velocity distribution function $W(v_z)$:

$$n_\alpha(v_z)\,dv_z = W(v_z)\,\Lambda_\alpha dv_z, \qquad (24)$$

where $n_\alpha(v_z)\,dv_z$ is the number of atoms in the velocity interval $(v_z,\,v_z+dv_z)$ excited in state α.

Consider one atom with axial velocity v_z. When excited at a point z_0, at an instant t_0, at a sublevel α, its dipole moment $\mathbf{p}(v_z,\,z,\,t)$ at t and $z=z_0+v_z(t-t_0)$ is known once its wave function $\psi(v_z,\,z,\,t)$ is known. Let

$$\psi(v_z,\,z,\,t) = \sum_{m=-j_a}^{+j_a} a_m\psi_{a_m} + \sum_{m=-j_b}^{+j_b} b_m\psi_{b_m}, \qquad (25)$$

by substitution of (25) we then find the dipole moment to be

$$\mathbf{p}(v_z,\,z,\,t) \equiv \int \psi^{*}(v_z,\,z,\,t)\,e\mathbf{r}\psi(v_z,\,z,\,t)\,d\tau$$

$$= \tfrac{1}{2}\sum_{m=-j_a}^{+j_a}\left[\rho_{a_mb_{m+1}}p_{m,m+1}(\mathbf{x}-i\mathbf{y}) + \rho_{a_mb_{m-1}}p_{m,m-1}(\mathbf{x}+i\mathbf{y})\right]+\text{c.c.}, \qquad (26)$$

where we introduce the density matrix elements

$$\rho_{a_mb_{m'}} = \rho_{a_mb_{m'}}[\alpha,\,v_z,\,z-v_z(t-t_0),\,t_0;\,t] = a_mb_{m'}{}^{*}, \qquad (27)$$

being density matrix elements at time t for an atom with velocity v_z, excited at $z_0=z-v_z(t-t_0)$ at t_0 in state α. The macroscopic polarization vector can then easily be written as follows:

$$\mathbf{P}(z,\,t) = \tfrac{1}{2}\sum_{\alpha=a_k,b_k}\Lambda_\alpha\int_{-\infty}^{+\infty}dv_z W(v_z)$$

$$\times\int_{-\infty}^{t}dt_0\sum_{m=-j_a}^{+j_a}\{\rho_{a_mb_{m+1}}[\alpha,\,v_z,\,z-v_z(t-t_0),\,t_0;\,t]p_{m,m+1}(\mathbf{x}-i\mathbf{y}) + \rho_{a_mb_{m-1}}[\alpha,\,v_z,\,z-v_z(t-t_0),\,t_0;\,t]p_{m,m-1}(\mathbf{x}+i\mathbf{y})\}+\text{c.c.}$$

$$(28)$$

The wave function (25) fulfils the Schrödinger equation with (21) as a perturbation Hamiltonian. The Schrödinger equation, extended with spontaneous decay terms, can be written as a set of $2(j_a+j_b+1)$ coupled equations:

$$i\dot{a}_k = (\omega_{a_k}-\tfrac{1}{2}i\gamma_a)a_k + V_t(a_k,\,b_{k+1})b_{k+1} + V_t(a_k,\,b_{k-1})b_{k-1}, \qquad (29a)$$

$$i\dot{b}_l = (\omega_{b_l}-\tfrac{1}{2}i\gamma_b)b_l + V_t{}^{*}(a_{l+1},\,b_l)a_{l+1} + V_t{}^{*}(a_{l-1},\,b_l)a_{l-1}. \qquad (29b)$$

They are to be solved by iteration in the desired order in the fields. It is convenient, however, to derive from (29) an equivalent set of equations for the density matrix

$$i\dot{\rho}_{a_kb_l} = [\omega_{a_k}-\omega_{b_l}-i\gamma_{ab}]\rho_{a_kb_l} + \sum_{h=\pm1}[V_t(a_k,\,b_{k+h})\rho_{b_{k+h}b_l} - V_t(a_{l+h},\,b_l)\rho_{a_ka_{l+h}}], \qquad (30)$$

$$i\dot{\rho}_{a_ka_l} = [\omega_{a_k}-\omega_{a_l}-i\gamma_a]\rho_{a_ka_l} + \sum_{h=\pm1}[V_t(a_k,\,b_{k+h})\rho_{b_{k+h}a_l} - V_t{}^{*}(a_l,\,b_{l+h})\rho_{a_kb_{l+h}}], \qquad (31)$$

$$i\dot{\rho}_{b_kb_l} = [\omega_{b_k}-\omega_{b_l}-i\gamma_b]\rho_{b_kb_l} + \sum_{h=\pm1}[V_t{}^{*}(a_{k+h},\,b_k)\rho_{a_{k+h}b_l} - V_t(a_{l+h},\,b_l)\rho_{b_ka_{l+h}}], \qquad (32)$$

where

$$\rho_{a_k a_l} = a_k a_l^*; \qquad \rho_{b_k b_l} = b_k b_l^*. \tag{33}$$

The iteration procedure leading to expressions for ρ in the third order in the **E** field and the specialization on terms in the zeroth and first order in the external **H** field is outlined in Appendix B. The respective velocity integrations are dealt with in Appendix C. We finish with an expression for the third-order **P** vector valid when the Zeeman splitting is much smaller than the decay constants γ_a and γ_b.

The absorptive parts of the **P** vector are calculated in the Doppler limit, except for a (magnetic-field-induced) absorptive part, in which the slope of the Doppler profile enters (see the α' coefficient).

The first-order dispersive parts largely depend on the full shape of the Doppler profile.

Besides giving contributions in the Doppler limit, the third-order dispersive parts give contributions pro-portional to the slope of the Doppler profile, which may be of comparable size, far from line center.

The resulting **P** vector is given by writing down the explicit expressions for the twelve phenomenological constants in Eqs. (7) and (8). All twelve constants are proportional to the "excitation density."

$$N = \Lambda_a/\gamma_a - \Lambda_b/\gamma_b, \tag{34}$$

where, in the absence of oscillations Λ_a/γ_a is the density of atoms in any sublevel a_k, while Λ_b/γ_b is the same for any sublevel b_k. Sums over matrix elements run from $m = -j_a$ to $+j_a$. We write $\omega_a - \omega_b = \omega$, and intro-duce the notation

$$\mathcal{L}(\omega - \nu) = [(\omega - \nu)^2 + \gamma_{ab}^2]^{-1}. \tag{35}$$

The twelve constants follow from the analysis in Appendices B and C:

$$\alpha = (\pi\nu/2\epsilon_0\hbar K) N W[(\omega-\nu)/K] \sum_m p_{m,m+1}^2, \tag{36}$$

$$\sigma = \alpha \left[-\pi^{-1} \int_{-\infty}^{+\infty} d\nu' \frac{\nu' W[(\omega-\nu+\nu')/K]}{(\nu'^2+\gamma_{ab}^2) W[(\omega-\nu)/K]} \right] \equiv \alpha J_1, \tag{37}$$

$$\alpha' = (\pi\nu/2\epsilon_0\hbar K) N (dW/dv)_{v=(\omega-\nu)/K} (\mu_B/\hbar) \left[g_b \sum_m p_{m,m+1}^2 - (g_a-g_b) \sum_m p_{m,m+1}^2 m \right], \tag{38}$$

$$\sigma' = \alpha \left[\pi^{-1} \int_{-\infty}^{+\infty} d\nu' \frac{(\nu'^2-\gamma_{ab}^2) W[(\omega-\nu+\nu')/K]}{(\nu'^2+\gamma_{ab}^2) W[(\omega-\nu)/K]} \right] (\mu_B/\hbar) \left[-g_b + (g_a-g_b) \frac{\sum_m p_{m,m+1}^2 m}{\sum_m p_{m,m+1}^2} \right]$$

$$\equiv \alpha J_2(\mu_B/\hbar) \left[-g_b + (g_a-g_b) \left(\sum_m p_{m,m+1}^2 m / \sum_m p_{m,m+1}^2 \right) \right], \tag{39}$$

$$\beta_1 = (\pi\nu/16\epsilon_0\hbar^3 K\gamma_a\gamma_b) N W[(\omega-\nu)/K][(\omega-\nu)^2+2\gamma_{ab}^2]\mathcal{L}(\omega-\nu) \sum_m p_{m,m+1}^4, \tag{40}$$

$$\rho_1 = \beta_1 \mathcal{L}^{-1}(\omega-\nu)[(\omega-\nu)^2+2\gamma_{ab}^2]^{-1} \left[\gamma_{ab}(\omega-\nu)\mathcal{L}(\omega-\nu) - \frac{\gamma_{ab}(dW/dv)_{v=(\omega-\nu)/K}}{KW[(\omega-\nu)/K]} \right], \tag{41}$$

$$\beta_2 = \beta_1 \left(\sum_m [p_{m+2,m+1}^2 p_{m,m+1}^2 + p_{m,m-1}^2 p_{m,m+1}^2] / \sum_m p_{m,m+1}^4 \right), \tag{42}$$

$$\rho_2 = \rho_1(\beta_2/\beta_1), \tag{43}$$

$$\beta'_1 = (\pi\nu\gamma_{ab}^2/4\epsilon_0\hbar^3 K\gamma_a\gamma_b) N W[(\omega-\nu)/K](\omega-\nu)\mathcal{L}^2(\omega-\nu) (\mu_B/\hbar) \left[g_b \sum_m p_{m,m+1}^4 - (g_a-g_b) \sum_m p_{m,m+1}^4 m \right], \tag{44}$$

$$\rho'_1 = (\pi\nu\gamma_{ab}/8\epsilon_0\hbar^3 K\gamma_a\gamma_b) N W[(\omega-\nu)/K][(\omega-\nu)^2-\gamma_{ab}^2]\mathcal{L}^2(\omega-\nu) (\mu_B/\hbar) \left[g_b \sum_m p_{m,m+1}^4 - (g_a-g_b) \sum_m p_{m,m+1}^4 m \right], \tag{45}$$

$$\beta'_2 = (\pi\nu/8\epsilon_0\hbar^3 K\gamma_a\gamma_b) N W[(\omega-\nu)/K](\omega-\nu)\mathcal{L}(\omega-\nu) (\mu_B/\hbar) [g_a\{\gamma_{ab}(\gamma_a+2\gamma_b)\mathcal{L}(\omega-\nu)+\gamma_b\gamma_a^{-1}\}$$

$$\times \sum_m p_{m+2,m+1}^2 p_{m,m+1}^2 + g_b(\{\gamma_{ab}\gamma_a\mathcal{L}(\omega-\nu)+\gamma_a\gamma_b^{-1}\} \sum_m p_{m,m+1}^2 p_{m,m-1}^2 - 2\gamma_{ab}^2\mathcal{L}(\omega-\nu) \sum_m p_{m+2,m+1}^2 p_{m,m+1}^2)$$

$$-2(g_a-g_b)\gamma_{ab}^2\mathcal{L}(\omega-\nu) \sum_m (p_{m,m+1}^2 p_{m,m-1}^2 + p_{m+2,m+1}^2 p_{m,m+1}^2) m], \tag{46}$$

$$\rho'_2 = (\pi\nu/8\epsilon_0\hbar^3 K\gamma_a\gamma_b) N W[(\omega-\nu)/K](\mu_B/\hbar) [g_a\{(\gamma_{ab}+\gamma_b)[(\omega-\nu)^2-\gamma_{ab}^2]\mathcal{L}^2(\omega-\nu) - \gamma_{ab}\gamma_b\gamma_a^{-1}\mathcal{L}(\omega-\nu) - 2\gamma_a^{-1}\}$$

$$\times \sum_m p_{m+2,m+1}^2 p_{m,m+1}^2 + g_b\{(\tfrac{1}{2}\gamma_a[(\omega-\nu)^2-\gamma_{ab}^2]\mathcal{L}^2(\omega-\nu) - \gamma_{ab}\gamma_a\gamma_b^{-1}\mathcal{L}(\omega-\nu) - 2\gamma_b^{-1})$$

$$\times \sum_m p_{m,m+1}^2 p_{m,m-1}^2 - \gamma_{ab}[(\omega-\nu)^2-\gamma_{ab}^2]\mathcal{L}^2(\omega-\nu) \sum_m p_{m+2,m+1}^2 p_{m,m+1}^2\} - (g_a-g_b)\gamma_{ab}[(\omega-\nu)^2-\gamma_{ab}^2]\mathcal{L}^2(\omega-\nu)$$

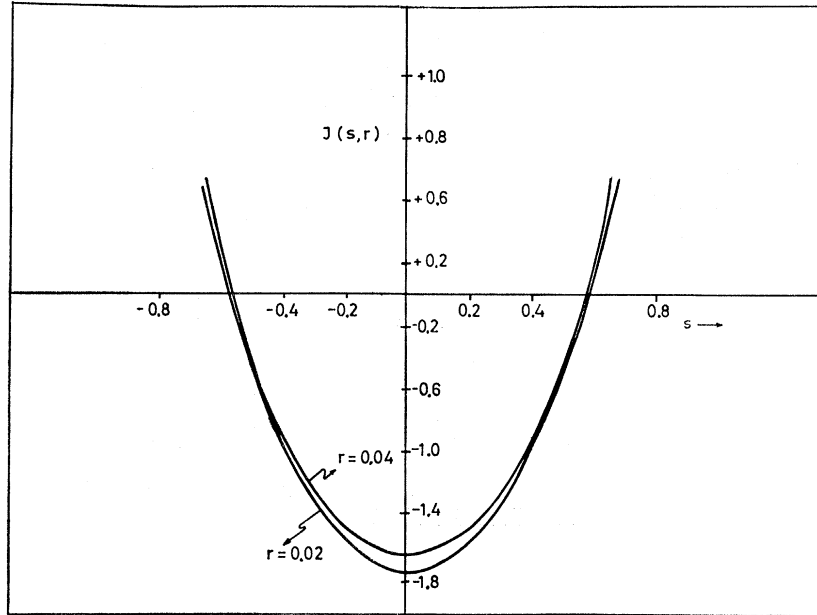$$\times \{\sum_m (p_{m,m+1}^2 p_{m,m-1}^2 + p_{m+2,m+1}^2 p_{m,m+1}^2) m\}]. \tag{47}$$

FIG. 1. $J(s, r)$ [Eq. (49)] as a function of $s = (\omega - \nu)/\gamma_D$ for $r = \gamma_{ab}/\gamma_D = 0.02$ and 0.04.

Both of the two velocity integrals J_1 and J_2 entering in the dispersive coefficients σ and σ' largely depend on the full shape of $W(v)$. We do not calculate J_1, as the σ coefficient does not enter into the equations of motion (13), (14), and (15). The coefficient σ', however, does. If we choose a Maxwellian distribution

$$W(v) = (u\pi^{1/2})^{-1} \exp[-v^2/u^2], \tag{48}$$

the J_2 integral in (39) is easily seen to be $\gamma_D^{-1}J(s, r)$, where

$$J(s, r) = \pi^{-1}\int_{-\infty}^{+\infty} dy \frac{(y^2 - r^2)}{(y^2 + r^2)^2} \exp[-4 (y^2 + 2sy)\ln 2], \tag{49}$$

γ_D is the Doppler width, $s = (\omega - \nu)/\gamma_D$, and $r = \gamma_{ab}/\gamma_D$. The function $J(s, r)$ is an even function of s. In Fig. 1, J is plotted as a function of s with $r = 0.02$ and 0.04.

We wish to specialize on the case of equal Landé factors $g_a = g_b$ (the more general case $g_a \neq g_b$ can in principle be handled). Therefore only a limited number of polarization sums are needed. They are calculated using the well-known expressions for the matrix elements.[16] Calling $j_a = j$ we find

$$\sum_m p_{m,m+1}^2 \equiv f_1(j)p^2 = \tfrac{2}{3}(2j+1)(j+1)jp^2, \qquad \text{for} \quad j \to j$$

$$= \tfrac{2}{3}(2j+1)(j+1)(2j+3)p^2, \quad \text{for} \quad j \leftrightarrow j+1 \tag{50}$$

$$\sum_m p_{m,m+1}^4 \equiv f_2(j)p^4 = \tfrac{4}{15}(2j+1)(j+1)(2j^2+2j+1)jp^4, \qquad \text{for} \quad j \to j$$

$$= \tfrac{4}{15}(2j+1)(j+1)(6j^2+12j+5)(2j+3)p^4, \quad \text{for} \quad j \leftrightarrow j+1 \tag{51}$$

$$\sum_m p_{m+2,m+1}^2 p_{m,m+1}^2 \equiv f_3(j)p^4 = \tfrac{2}{15}(2j+1)(j+1)(2j+3)(2j-1)jp^4, \quad \text{for} \quad j \to j \text{ and } j \to j+1$$

$$= \tfrac{2}{15}(2j+1)(j+1)(2j+3)(j+2)(2j+5)p^4 \quad \text{for} \quad j+1 \to j \tag{52}$$

$$\sum_m p_{m,m+1}^2 p_{m,m-1}^2 \equiv f_4(j)p^4 = \tfrac{2}{15}(2j+1)(j+1)(2j+3)(2j-1)jp^4, \quad \text{for} \quad j \to j \quad \text{and} \quad j+1 \to j$$

$$= \tfrac{2}{15}(2j+1)(j+1)(2j+3)(j+2)(2j+5)p^4, \quad \text{for} \quad j \to j+1, \tag{53}$$

where p is a reduced matrix element. The p can easily be related to the excitation and loss characteristics: Let $\bar{N}(\nu, \chi, \vartheta)$ be the critical excitation density at frequency ν for laser operation, i.e., the density for which

$$\alpha(\nu, \bar{N}) = \text{Re}\Gamma - h_3(\chi, \vartheta) \equiv G(\chi, \vartheta), \tag{54}$$

---

16 H. Weyl, *The Theory of Groups and Quantum Mechanics* (Dover Publications, Inc., New York).

where $G(\chi, \vartheta)$ is the χ- and ϑ-dependent loss of the empty cavity [far enough from threshold, the cavity term $|h_3(\chi, \vartheta)|$ will be much smaller than $\mathrm{Re}\Gamma$, implying a cavity loss G almost independent of χ and ϑ]. Introducing the excess excitation density

$$F(\nu, \chi, \vartheta) = N/\bar{N}(\nu, \chi, \vartheta) = \alpha(\nu, N)/G(\chi, \vartheta) \tag{55}$$

which also depends on ν, χ, and ϑ, we can write, according to (36)

$$p^2 = \{2\epsilon_0 \hbar K F G/\pi\nu N W[(\omega-\nu)/K]f_1(j)\}. \tag{56}$$

Specializing to the case of the Maxwellian distribution (48), and taking $g_a = g_b = g$, we finally obtain for the coefficients (36) to (47), abbreviating $F(\nu, \chi, \vartheta) = F$ and $G(\chi, \vartheta) = G$,

$$\alpha = FG, \tag{36'}$$

$$\sigma = FGJ_1, \tag{37'}$$

$$\alpha' = -8FGs \ln2(\mu_B g/\hbar\gamma_D), \tag{38'}$$

$$\sigma' = -FG(\mu_B g/\hbar\gamma_D)J(s, r), \tag{39'}$$

$$\beta_1 = \frac{FGp^2}{8\hbar^2\gamma_a\gamma_b}\left(\frac{s^2+2r^2}{s^2+r^2}\right)\frac{f_2(j)}{f_1(j)}, \tag{40'}$$

$$\rho_1 = \frac{FGp^2 rs}{8\hbar^2\gamma_a\gamma_b}\left(\frac{1+8(s^2+r^2)\ln2}{s^2+r^2}\right)\frac{f_2(j)}{f_1(j)}, \tag{41'}$$

$$\beta_2 = \beta_1(f_3(j)+f_4(j))/f_2(j), \tag{42'}$$

$$\rho_2 = \rho_1(f_3(j)+f_4(j))/f_2(j), \tag{43'}$$

$$\beta'_1 = \frac{FGp^2}{2\hbar^2\gamma_a\gamma_b}\frac{r^2s}{(s^2+r^2)^2}\frac{\mu_B g}{\hbar\gamma_D}\frac{f_2(j)}{f_1(j)}, \tag{44'}$$

$$\rho'_1 = \frac{FGp^2}{4\hbar^2\gamma_a\gamma_b}\frac{r(s^2-r^2)}{(s^2+r^2)^2}\frac{\mu_B g}{\hbar\gamma_D}\frac{f_2(j)}{f_1(j)}, \tag{45'}$$

$$\beta'_2 = \frac{FGp^2}{4\hbar^2\gamma_a\gamma_b}\frac{\mu_B g}{\hbar\gamma_D}\left[\left\{\frac{\gamma_b sr}{\gamma_D(s^2+r^2)^2}+\frac{\gamma_b s}{\gamma_a(s^2+r^2)}\right\}\frac{f_3(j)}{f_1(j)} + \left\{\frac{\gamma_a sr}{\gamma_D(s^2+r^2)^2}+\frac{\gamma_a s}{\gamma_b(s^2+r^2)}\right\}\frac{f_4(j)}{f_1(j)}\right], \tag{46'}$$

$$\rho'_2 = \frac{FGp^2}{4\hbar^2\gamma_a\gamma_b}\frac{\mu_B g}{\hbar\gamma_D}\left[\left\{\frac{\gamma_b(s^2-r^2)}{2\gamma_D(s^2+r^2)^2}-\frac{r\gamma_b}{\gamma_a(s^2+r^2)}-\frac{2\gamma_D}{\gamma_a}\right\}\frac{f_3(j)}{f_1(j)} + \left\{\frac{\gamma_a(s^2-r^2)}{2\gamma_D(s^2+r^2)^2}-\frac{r\gamma_a}{\gamma_b(s^2+r^2)}-\frac{2\gamma_D}{\gamma_b}\right\}\frac{f_4(j)}{f_1(j)}\right], \tag{47'}$$

where the expression (56) has to be substituted for p^2 in Eqs. (40')–(47'). By the introduction of F and G we thus finally arrive at expressions for the twelve coefficients in Eqs. (7) and (8), depending on both experimental and theoretical parameters, which are in principle all known. Inspection shows that α, σ', β_1, β_2, ρ'_1, and ρ'_2 are even in $s = (\omega-\nu)/\gamma_D$, whereas α', σ, ρ_1, ρ_2, β'_1, and β'_2 are odd in s.

We are now ready to discuss Eqs. (13)–(15).

IV. BEHAVIOR OF THE POLARIZATION PARAMETERS

A. Zero Magnetic Field; Isotropic Cavity

In the case of an isotropic cavity, i.e., $h_1(\chi, \vartheta) = h_2(\chi, \vartheta) = h_3(\chi, \vartheta) \simeq 0$, and a zero magnetic field, Eqs. (13)–(15), reduce to

$$d\chi/dt = \tfrac{1}{8}(\beta_2-\beta_1)I \sin4\chi, \tag{57}$$

$$\cos2\chi(d\vartheta/dt) = \tfrac{1}{8}(\rho_2-\rho_1)I \sin4\chi, \tag{58}$$

$$I^{-1}(dI/dt) = \alpha-\tfrac{1}{2}(\beta_1 I)(1+\sin^2 2\chi)-\tfrac{1}{2}(\beta_2 I)\cos^2 2\chi - \mathrm{Re}\Gamma. \tag{59}$$

If operating ($I>0$), the behavior of χ, according to (57), is largely dependent on the factor $(\beta_2-\beta_1)$. According to Eq. (42') we have

$$\beta_2-\beta_1 = \beta_1\{(f_3(j)+f_4(j))/f_2(j)-1\}, \tag{60}$$

where $\beta_1 > 0$. From (51)–(53), we find

$$(f_3(j) + f_4(j))/f_2(j) - 1 = 2(j^2 + j - 2)/(2j^2 + 2j + 1) \quad \text{for} \quad j \to j$$

$$= -4j(j+2)/(j^2 + 12j + 5) \quad \text{for} \quad j \leftrightarrow j + 1. \tag{61}$$

$(\beta_2 - \beta_1)$ is therefore negative when the atomic transition is either a $j = \frac{1}{2} \to j = \frac{1}{2}$ type transition, or a $j \leftrightarrow j + 1$ type transition $(j > 0)$; positive for $j \to j$ transitions $(j > 1)$; zero for $j = 0 \leftrightarrow j = 1$ and $j = 1 \to j = 1$ transitions. In the first case the mode becomes linearly polarized; in the second case it becomes right or left circularly polarized (bistable); in the third case there is no preference for any ellipticity.

Both tendencies towards linear and circular polarization have been reported for a variety of modes.[8,15] A well-known example is the He–Ne 1.153-μ mode, being of type $j = 1 \to j = 2$, showing linear preference. Circular preference has been observed for a $j = 2 \to j = 2$ transition in agreement with the above theory (the He–Ne 1.207-μ line[8]).

It seems that isolated $j = 0 \to j = 1$ transition laser modes show slight circular preference,[8,15] disagreeing with the above predictions. The small bistability in these cases is not understood. None of the existing theories has solved this problem.

B. Zero Magnetic Field; Anisotropic Cavity

In this case, Eqs. (13)–(15), read

$$d\chi/dt = \tfrac{1}{8}(\beta_2 - \beta_1)I \sin 4\chi + h_1(\chi, \vartheta), \tag{62}$$

$$\cos 2\chi (d\vartheta/dt) = \tfrac{1}{8}(\rho_2 - \rho_1)I \sin 4\chi + h_2(\chi, \vartheta), \tag{63}$$

$$I^{-1}(dI/dt) = \alpha - \tfrac{1}{2}(\beta_1 I)(1 + \sin^2 2\chi) - \tfrac{1}{2}(\beta_2 I)\cos^2 2\chi - \text{Re}\Gamma + h_3(\chi, \vartheta), \tag{64}$$

where h_1, h_2, and h_3 are given by (16)–(18), respectively. Assume that $a' = \phi' = 0$ (the effect of circular anisotropies is incorporated in a later stage). The asymptotic solution (for high enough intensity, excluding $0 \leftrightarrow 1$ and $1 \to 1$ transitions) of (62)–(64), is given by

$$d\chi/dt = \cos 2\chi (d\vartheta/dt) = I^{-1}(dI/dt) = 0. \tag{65}$$

The latter equation, using (54) and (55), gives

$$I = [4(F(\nu, \chi, \vartheta) - 1)G(\chi, \vartheta)/((3\beta_1 + \beta_2) + (\beta_2 - \beta_1)\cos 4\chi)], \tag{66}$$

being the asymptotic energy, which depends on the asymptotic χ and ϑ through F, G, and the $\cos 4\chi$ in the denominator. In general $0 < (F - 1) \lesssim 0.5$, whereas $LG/c \simeq 0.03$ per pass. Insertion of (66) in (62) and (63) gives (in the asymptotic state)

$$d\chi/dt = \tfrac{1}{2}[F(\nu, \chi, \vartheta) - 1]G(\chi, \vartheta)[S \sin 4\chi/(S \cos 4\chi + 1)] + h_1(\chi, \vartheta) = 0, \tag{67}$$

$$\cos 2\chi (d\vartheta/dt) = \tfrac{1}{2}[F(\nu, \chi, \vartheta) - 1]G(\chi, \vartheta)[TS \sin 4\chi/(S \cos 4\chi + 1)] + h_2(\chi, \vartheta) = 0. \tag{68}$$

where

$$S = [(j-1)(j+2)/5j(j+1)] \quad \text{for} \quad j \to j$$

$$= -[j(j+2)/5(j+1)^2] \quad \text{for} \quad j \leftrightarrow j + 1 \tag{69}$$

and

$$T = \rho_1/\beta_1 = [rs/(s^2 + 2r^2)][1 + 8(s^2 + 2r^2)\ln 2]. \tag{70}$$

The medium-induced absorptive anisotropic effect in (67) was derived by Polder and Van Haeringen.[6] As is seen in (68) there is an additional medium-induced effect on the phase. Both medium-induced effects have been calculated earlier by De Lang[17] for a phenomenological model, providing the same expressions, except for the explicit j dependence of S. The ratio of both medium-induced dispersive and absorptive anisotropic effects in (67) and (68) is equal to T. The T function is plotted in Fig. 2 as a function of s for the values $r = 0.02$ and $r = 0.04$. Equations (67) and (68) with h_1

and $h_2 \neq 0$ can be solved in principle, giving the asymptotic χ and ϑ values.

Let us specialize to the $j = 1 \to j = 2$ transition, for which $S = -\frac{3}{20}$. In this case the medium-induced anisotropy favors linear polarization (see Sec. IV. A) If the cavity has a linear phase anisotropy only $[h_1 = \frac{1}{2}\phi_0 \sin 2(\vartheta - \vartheta_2), h_2 = -\frac{1}{2}\phi_0 \cos 2(\vartheta - \vartheta_2) \sin 2\chi]$ the stable solution of (67) and (68) is given by $\chi = 0$; $\vartheta = \vartheta_2$. If the cavity has a linear absorption anisotropy only $[h_1 = \frac{1}{2}a \cos 2(\vartheta - \vartheta_1) \sin 2\chi, h_2 = \frac{1}{2}a \sin 2(\vartheta - \vartheta_1)]$ the stable solution is $\chi = 0$; $\vartheta = \vartheta_1$. A combination of both a linear phase and absorption anisotropy gives a stable χ value, which in general is different from zero.

[17] H. de Lang, thesis, University of Utrecht, 1966 (unpublished).

FIG. 2. The ratio $T=$ ρ_1/β_1 of dispersive and absorptive nonlinear coefficients, as a function of $s=(\omega-\nu)/\gamma_D$ for the values 0.02 and 0.04 of the parameter $r=\gamma_{ab}/\gamma_D$. The dotted lines represent the contribution due to hole-hole interaction. The solid lines are found if the nonlinear dispersive effects, originating from the local slope in the velocity distribution, are taken into account. The effects in the local slope have been ignored in the work of Lamb (Ref. 7).
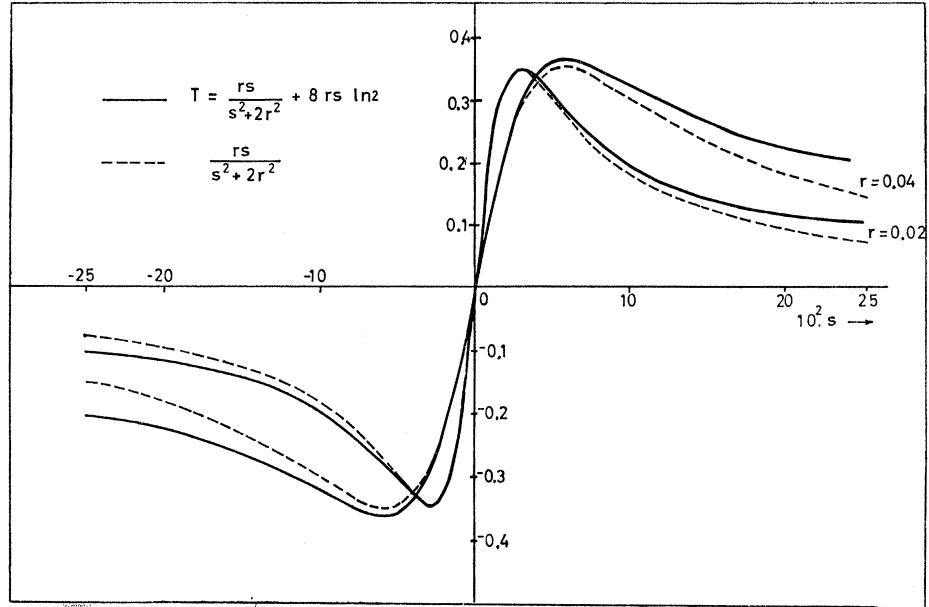
In practice we have linear phase and absorption anisotropies, which are very small.[18] However, where $(F-1)$ is small enough the cavity terms in (67) and (68) can nevertheless be dominant in the determination of the stable χ and ϑ values. In the experiments on the He–Ne 1.153-μ mode, referred to in the Introduction, the polarization is always linear. This implies a high enough $(F-1)$ to reduce all cavity or magnetic-field effects on the ellipticity χ. In order to guarantee linear polarization, $(F-1)$ should not be too small. More precisely, in order to have $|\chi| \leq |\chi_0| \ll \pi/4$, the excess excitation density should fulfil

$$F(\nu, \chi, \vartheta) - 1 \gtrsim \delta > 0, \tag{71}$$

where δ of course depends on $|\chi_0|$, a, ϕ_0, and external magnetic fields. In practice δ is about 0.1. As F decreases monotonically as $|\omega-\nu|$ increases, condition (71) implies in general a restricted frequency range (if at all) around line center.

Furthermore, where the cavity anisotropy is small enough, we have

$$G(\chi, \vartheta) = \text{Re}\Gamma - h_3(\chi, \vartheta) \simeq \text{Re}\Gamma. \tag{72}$$

Taking $LG/c = 3 \times 10^{-2}$ per pass and $L |h_3|/c < 3 \times 10^{-5}$ per pass, which are reasonable numbers, the error is at most 0.1%. G can thus be considered to be independent of χ and ϑ. The same applies to F [see Eq. (55)]. From this $(F-1)$ can be considered to be independent of χ and ϑ, the error being at most 1%.

C. Small Axial Magnetic Field; Anisotropic Cavity

We now discuss the full Eqs. (13)–(15). The magnetic field is subject to the condition

$$\mu_B g |\mathbf{H}| \ll \hbar\gamma_a, \hbar\gamma_b. \tag{73}$$

[18] Th. Hänsch and P. Toschek, Phys. Letters 22, 150 (1966).

The main effect of this field will be on the phase difference ϑ. If $(F-1) > 0.1$, magnetic fields of at most 1 Oe [see (73)] are incapable of changing the ellipticity χ appreciably. This follows from a comparison between the respective medium- and magnetic-field-induced terms in Eq. (13). Take for instance

$$\mu_B g |\mathbf{H}|/\hbar = 2 \text{ Mc/sec}; \qquad \gamma_D = 1000 \text{ Mc/sec};$$

$$\gamma_{ab} = 40 \text{ Mc/sec}; \qquad |\omega-\nu| = 200 \text{ Mc/sec};$$

$$S = -\tfrac{3}{20}; \qquad F = 1.1; \qquad LG/c = 0.03$$

per pass, and $h_1 = 0$. The ratio of both terms is then found to be

$$\left| \frac{\tfrac{1}{8}(\beta_2-\beta_1)I \sin4\chi}{\tfrac{1}{2}H_z a' \cos2\chi} \right| = 12.8 |\sin2\chi|, \tag{74}$$

which is equal to 1 in the equilibrium situation. This leads to $|\chi| \simeq 0.04$ rad. With increasing $(F-1)$ the χ values decrease in inverse proportion to $(F-1)$. The (nonlinear) magnetic-field term $\tfrac{1}{4}H_z(\beta'_1+\beta'_2)I \cos2\chi$ in (13) does not change the above picture.

The magnetic-field term in the intensity equation (15) is ignored. In the above numerical example it is at least fifty times smaller than $\alpha - \text{Re}\Gamma = (F-1)G$.

If we now try to solve Eqs. (13)–(15), in the magnetic-field case, allowing for a general cavity anisotropy (including small circular anisotropies) the first important observation is that there is an asymptotic energy value [see (66)] which is independent on χ, ϑ, and the magnetic-field

$$I = 2(F-1)G/(\beta_1+\beta_2), \tag{75}$$

where we write $\cos4\chi \simeq 1$. This energy is frequency-dependent (it shows the "Lamb dip"[7]). Insertion of (75) in (13) and (14) leads to two coupled equations

(taking $\sin 4\chi \simeq 4\chi$; $\cos 2\chi \simeq \cos 4\chi \simeq 1$):

$$\frac{d\chi}{dt} = \frac{2(F-1)GS\chi}{(S+1)} + \tfrac{1}{2}H_z\left(\alpha' + \frac{(F-1)G(\beta'_1+\beta'_2)}{(\beta_1+\beta_2)}\right) + a\chi \cos 2(\vartheta-\vartheta_1) + \tfrac{1}{2}\phi_0 \sin 2(\vartheta-\vartheta_2) + \tfrac{1}{2}a', \tag{76}$$

$$\frac{d\vartheta}{dt} = \frac{2(F-1)GST\chi}{(S+1)} + \tfrac{1}{2}H_z\left(\sigma' + \frac{(F-1)G(\rho'_1+\rho'_2)}{(\beta_1+\beta_2)}\right) + \tfrac{1}{2}a \sin 2(\vartheta-\vartheta_1) - \phi_0\chi \cos 2(\vartheta-\vartheta_2) - \tfrac{1}{2}\phi'. \tag{77}$$

A first type of solution is characterized by $d\chi/dt = d\vartheta/dt = 0$. It is obtained for relatively low magnetic fields. In this case, Eqs. (76) and (77) can be solved exactly. A second type of solution is obtained for relatively large magnetic fields. The angle ϑ is unstable then, and the plane of polarization will rotate in a nonuniform way [see (77)]. In the latter case, as long as condition (73) applies, the angle χ is very small depending smoothly on ϑ. Therefore, $|d\chi/dt| \ll |d\vartheta/dt|$, the ratio being of the order $2|\chi|_{\max}/\pi$. In this case we cannot give an exact solution to (76) and (77), but a nearly correct equation for $d\vartheta/dt$ can be obtained if we put $d\chi/dt = 0$. [In fact, this approximation is a first step in an iteration procedure, solving (76) and (77) for the case of an unstable polarization plane.] Thus in the cases of both stable and unstable polarization plane we use $d\chi/dt = 0$, or

$$\chi = \frac{-\tfrac{1}{2}\phi_0 \sin 2(\vartheta-\vartheta_2) - \tfrac{1}{2}a' - \tfrac{1}{2}H_z[\alpha' + (F-1)G(\beta'_1+\beta'_2)/(\beta_1+\beta_2)]}{2(F-1)GS/(S+1)}, \tag{78}$$

where we omitted the a-dependent term, which is permitted with $(F-1) > 0.1$ if $L|a|/c \ll 10^{-3}$ per pass. Insertion of (78) in (77) gives the desired equation for the angle

$$\frac{d\vartheta}{dt} = -\tfrac{1}{2}T\phi_0 \sin 2(\vartheta-\vartheta_2) + \frac{\phi_0^2(S+1)}{8(F-1)GS}\sin 4(\vartheta-\vartheta_2) + \frac{a'\phi_0(S+1)}{4(F-1)GS}\cos 2(\vartheta-\vartheta_2) + \tfrac{1}{2}a \sin 2(\vartheta-\vartheta_1) + \tfrac{1}{2}Ta' - \tfrac{1}{2}\phi'$$

$$+ \tfrac{1}{2}H_z\left[\sigma' + \frac{(F-1)G(\rho'_1+\rho'_2)}{(\beta_1+\beta_2)} - \left\{\alpha' + \frac{(F-1)G(\beta'_1+\beta'_2)}{(\beta_1+\beta_2)}\right\}\left\{T - \frac{\phi_0(S+1)}{2(F-1)GS}\cos 2(\vartheta-\vartheta_2)\right\}\right]. \tag{79}$$

In the next section Eq. (79) is applied to the He–Ne 1.153-μ mode.

V. POLARIZATION PHENOMENA IN WEAK MAGNETIC FIELDS

A. Isotropic Cavity; a, ϕ_0, a', $\phi' = 0$

Inserting the expressions from Sec. III for σ', α', ρ'_1, ρ'_2, β_1, β'_1, β_2, β'_2, we find in this case (magnetic-field term only)

$$d\vartheta/dt = G(\mu_B g H_z/\hbar\gamma_D)M(F, s, r, \gamma_a, \gamma_b, \gamma_D, j), \tag{80}$$

where

$$M = M_F + M_{F-1}[1] + M_{F-1}[2], \tag{81}$$

with

$$M_F = -\tfrac{1}{2}F[J(s,r) - 8sT\ln 2], \tag{82}$$

$$M_{F-1}[1] = (F-1)[f_2(j) + f_3(j) + f_4(j)]^{-1}f_2(j)(s^2+2r^2)^{-1}(s^2+r^2)^{-1}(rs^2-r^3-2r^2sT), \tag{83}$$

$$M_{F-1}[2] = (F-1)[f_2(j) + f_3(j) + f_4(j)]^{-1}(s^2+2r^2)^{-1}(s^2+r^2)^{-1}$$

$$\times[\{\tfrac{1}{2}\gamma_b\gamma_D^{-1}(s^2-r^2-2rsT) - \gamma_b\gamma_a^{-1}(s^2+r^2)(r-sT) - 2\gamma_D\gamma_a^{-1}(s^2+r^2)^2\}f_3(j)$$

$$+ \{\tfrac{1}{2}\gamma_a\gamma_D^{-1}(s^2-r^2-2rsT) - \gamma_a\gamma_b^{-1}(s^2+r^2)(r-sT) - 2\gamma_D\gamma_b^{-1}(s^2+r^2)^2\}f_4(j)], \tag{84}$$

which is valid only for $j \leftrightarrow j+1$ transitions ($j > 0$) or a $j = \tfrac{1}{2} \to j = \tfrac{1}{2}$ transition. The (dimensionless) M function is written as the sum of three parts M_F, $M_{F-1}[1]$, and $M_{F-1}[2]$. The M_F function is proportional to F. It has a (major) contribution from the field-induced dispersive part of the $P^{(1)}$ vector, and a (minor) contribution originating from the field-induced absorptive part of $P^{(1)}$. The latter absorptive part causes χ to be different from zero [see Eq. (78)], and therefore has

an effect on θ [see Eq. (79)]. The M_{F-1} functions are proportional to $(F-1)$. They have quite similar contributions originating from $P^{(3)}$. A distinction is made between $M_{F-1}[1]$ and $M_{F-1}[2]$. The $M_{F-1}[1]$ function consists of contributions originating from the ρ'_1 and β'_1 coefficients (and therefore excludes the effects of coupling of right- and left-circular parts of the mode). The $M_{F-1}[2]$ function contains contributions originating from ρ'_2 and β'_2 (it contains the
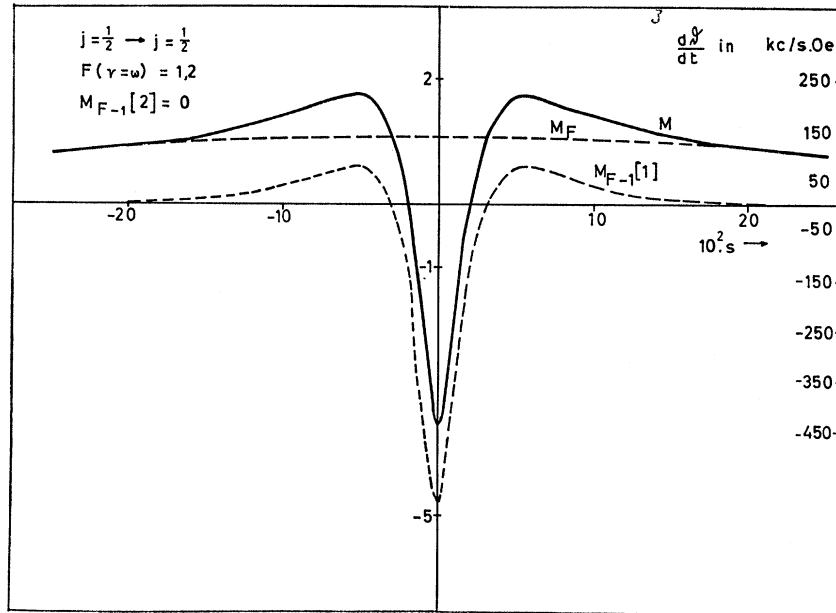
FIG. 3. M, M_F, and M_{F-1} [1] [Eqs. (81), (82), and (83)] as functions of s for $F=1.2$; $\gamma_{ab}=20$, $\gamma_a=4$, $\gamma_b=36$, $\gamma_D=1000$ Mc/sec. The atomic transition is $j=\frac{1}{2}\to j=\frac{1}{2}$. The corresponding $d\vartheta/dt$ is indicated (taking $G=0.03$ per pass of length $L=24$ cm) in kc/sec per Oe.

effects of coupling). In Figs. 3 and 4 the M functions are plotted as functions of s for a $j=\frac{1}{2}\to j=\frac{1}{2}$ and a $j=1\to j=2$ transition, respectively. The excitation parameter F is 1.2 at line center in both cases. Furthermore, $\gamma_D=1000$; $\gamma_{ab}=20$; $\gamma_a=4$; $\gamma_b=36$ Mc/sec. The duty cycle (i.e., the frequency region where $F>1$) is about 500 Mc/sec in this example. The M_F function (independent of the type of transition) is almost constant over the whole frequency region. It causes the plane of polarization to rotate in a positive direction around the **H** vector. The M_{F-1}[1] function is

large in the vicinity of the line center only, due to hole–hole interaction effects. In the direct neighborhood of the line center its sign is opposite to that of M_F. The contributions to M_{F-1}[2] are of a quite different nature. The (negative) contributions are quite large in the whole duty cycle. The reason for this is that, in the case of coupling, the magnetic field induces another type of dispersive effect arising from the non-diagonal second-order density matrix elements $\rho_{a_i a_j}{}^{(2)}$ and $\rho_{b_i b_j}{}^{(2)}$ (in the case of no coupling, only the diagonal $\rho_{a_i a_i}{}^{(2)}$ and $\rho_{b_i b_i}{}^{(2)}$ are relevant and give rise to hole–hole
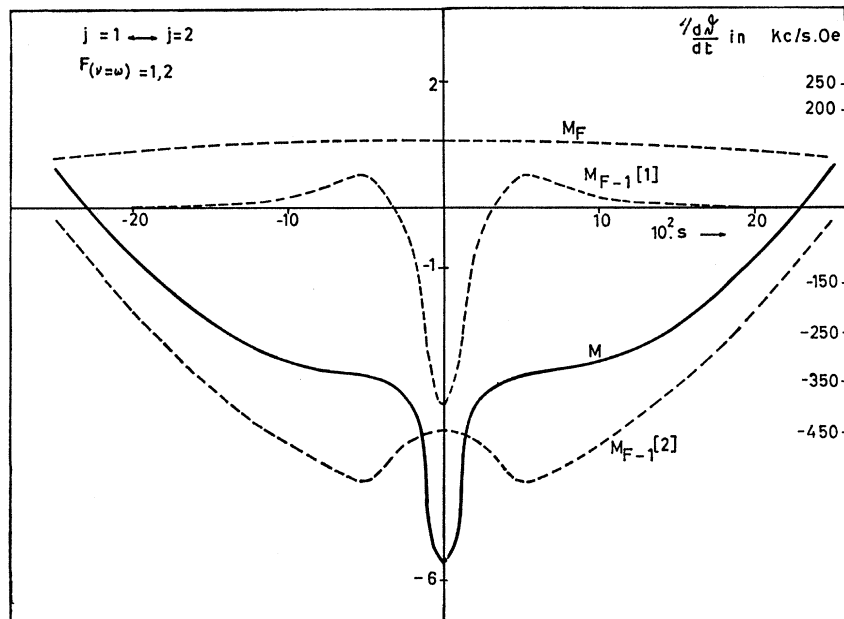

FIG. 4. M, M_F, M_{F-1} [1], and M_{F-1} [2] [Eqs. (81), (82), (83), and (84)] as functions of s for $F=1.2$; $\gamma_{ab}=20$, $\gamma_a=4$, $\gamma_b=36$, $\gamma_D=1000$ Mc/sec. The atomic transition is $j=1\to j=2$. The corresponding $d\vartheta/dt$ is indicated (taking $G=0.03$ per pass of length $L=24$ cm) in kc/sec per Oe.

interaction). In the calculation of $\mathbf{P}^{(3)}$ (Appendices B and C) this shows up in the appearance of denominators of the kind

$$[\gamma_b + i(\omega_{a_k} - \omega_{a_k \mp 2})]^{-1} \simeq \gamma_b^{-1}[1 \mp 2i\mu_B g H_z / \hbar \gamma_b], \quad (85)$$

and similar denominators with a and b interchanged. Dispersive effects originating from these denominators have a much slighter frequency dependence than the dispersive effects originating from hole–hole interaction.

In Figs. 3 and 4 the M_F and M_{F-1} functions are added to give the total M function. At first sight this seems to make no sense, the (third-order) M_{F-1} functions being larger than the (first-order) M_F. However, the convergence is better than one would think, looking at Figs. 3 and 4. This is due to the fact that hole–hole interaction, as well as the above indicated field-induced dispersive effect, begins to appear in the third order. Higher-order contributions to these effects are relatively small compared to the third-order contributions (the convergence is about as quick as in the case of the mode intensity). Though higher-order contributions could very well be of the order of M_F, the M function drawn in Figs. 3 and 4 certainly has some relevance.

The M function is rather sensitive to changes in F and the lifetimes γ_a^{-1} and γ_b^{-1}, as is seen from (81) to (84).

A final remark should be made concerning the possible effect of gas pressure on the above arguments. It is known that the effect of pressure is to decrease lifetimes and furthermore to redistribute sublevel populations.[18] The latter effect might very well reduce the relevance of the $M_{F-1}[2]$ part of the M function. The experimental work of Bolwijn[19] on He–Ne lasers with different gas pressure and excitation level in an axial magnetic field suggests that the effect of $M_{F-1}[2]$ is present at low pressures (1.7 mm Hg), whereas it is absent at higher pressures (6 and 9.2 mm Hg), though in these experiments **H** is outside the region (73).

B. Linear Absorption Anisotropy; ϕ_0, a', $\phi' = 0$

Equation (79) reads

$$d\vartheta/dt = \tfrac{1}{2}a \sin 2(\vartheta - \vartheta_1) + G(\mu_B g H_z / \hbar \gamma_D) M. \quad (86)$$

The ϑ, solving (86), fulfils

$$\sin 2(\vartheta - \vartheta_1) = (2G\mu_B g H_z / a\hbar \gamma_D) M \equiv A, \quad (87)$$

if $|A| \leq 1$, i.e., for small enough H_z fields. There are two solutions in this case, only one of them being stable. For $H_z = 0$ the solutions (mod. π) are $\vartheta = \vartheta_1$ and $\vartheta = \vartheta_1 + \tfrac{1}{2}\pi$. The former is stable if $a < 0$, the latter if $a > 0$. Increasing $|H_z|$ gives solutions [see (87)], that change continuously with H_z. A critical H_z value is reached when $\sin 2(\vartheta - \vartheta_1) = \pm 1$, giving stable solutions

[18] P. T. Bolwijn, in *Proceedings of the Physics of Quantum Electronics Conference, San Juan, Puerto Rico, 1965*, edited by P. L. Kelley, B. Lax, and P. E. Tannenwald (McGraw-Hill Book Company, Inc., New York, 1965).

$\vartheta = \vartheta_1 \pm \tfrac{1}{4}\pi$ (the sign depending on the sign of the field). The critical-field splitting is given by

$$| \mu_B g (H_z)_{\text{crit.}} / \hbar | = | \gamma_D a / 2GM |. \quad (88)$$

Taking $\gamma_D = 1000$ Mc/sec; $G = 0.03$, and $M = 1$, it is found that a critical-field splitting of 1 Mc/sec could be caused by a linear absorption anisotropy of about 6.10^{-5} per pass. The critical field is of course dependent on the frequency (through M), and can adopt much higher values in those regions where M is close to zero. For fields in excess of the critical value a nonuniform rotation occurs for ϑ. The zero-field solutions ($\vartheta = \vartheta_1$ or $\vartheta = \vartheta_1 + \tfrac{1}{2}\pi$) are completely independent of the frequency. In particular, tuning the laser through the center of the Doppler profile gives no change in the stable solution. Neither the polarization flip nor the observed hysteresis effect[4] at $H_z = 0$ can be explained, therefore, assuming a cavity which is purely absorption anisotropic.

C. Linear Phase Anisotropy; a, a', $\phi' = 0$

Equation (79) reads

$$d\vartheta/dt = -\tfrac{1}{2}T\phi_0 \sin 2(\vartheta - \vartheta_2)$$
$$+ \frac{\phi_0^2(S+1)}{8(F-1)GS} \sin 4(\vartheta - \vartheta_2) + G\frac{\mu_B g H_z}{\hbar \gamma_D} M, \quad (89)$$

where the term proportional to $\cos 2(\vartheta - \vartheta_2)$ is omitted. For not too high an s (and not too large a ϕ_0) this is permitted, as can easily be checked.

The magnetic-field term in (89) is equal to that in (86). The cavity terms, however, are quite different. Let $H_z = 0$. We then find

$$\sin 2(\vartheta - \vartheta_2) \left[-\tfrac{1}{2}T\phi_0 + \frac{\phi_0^2(S+1)}{4(F-1)GS} \cos 2(\vartheta - \vartheta_2) \right] = 0. \quad (90)$$

Equation (90) has the two solutions: $\vartheta = \vartheta_2$; $\vartheta = \vartheta_2 + \tfrac{1}{2}\pi$, and possibly the two solutions of

$$\cos 2(\vartheta - \vartheta_2) = 2(F-1)GST/\phi_0(S+1) \equiv B, \quad (91)$$

if $|B| \leq 1$. The last two solutions exist only in the direct neighborhood of $s = 0$ (line center) and are both unstable.

In the small s region around line center where

$$| -\tfrac{1}{2}T\phi_0 | < | \phi_0^2(S+1)/4(F-1)GS |, \quad (92)$$

both the $\vartheta = \vartheta_2$ and $\vartheta = \vartheta_2 + \tfrac{1}{2}\pi$ solutions are stable, the factor in the brackets of (90) being negative in the first case and positive in the second case. At a higher s the inequality (92) no longer applies, leading to one stable solution only. As the factor $-\tfrac{1}{2}T\phi_0$ changes sign if we replace s by $-s$, the stable ϑ solution for positive s differs $\tfrac{1}{2}\pi$ from that for negative s. The region of bistability is easily found from (92). Taking $|\phi_0| = 3.10^{-4}$ rad per pass; $(F-1) = 0.2$; $G = 0.03$ per pass; $S = -\tfrac{3}{20}$, $r = 0.02$, the maximum $|s|$ for which the

inequality (92) holds is 0.07. Taking $\gamma_D = 1000$ Mc/sec this gives a bistability region of about 14 Mc/sec.

Thus both the polarization flip at the line center and the small region of bistability[4] are found at $H_z = 0$. The $H_z \neq 0$ case is easy to discuss for those frequencies where the $\sin 4(\vartheta - \vartheta_2)$ term is small compared to the $\sin 2(\vartheta - \vartheta_2)$ term. In that case we once more find (see Sec. V. B) that there is a stable polarization plane for sufficiently small fields. A critical-field splitting is found for which the position of the plane of polarization differs by $\pm \frac{1}{4}\pi$ from the position at zero field. The critical-field splitting is in this case found from

$$| \mu_B g(H_z)_{\text{crit.}}/\hbar | = | \gamma_D T \phi_0/2GM |. \qquad (93)$$

Taking the same example as in (Sec. V. B), with $T \simeq 0.2$, we find that critical-field splittings of 1 Mc/sec can be caused by a linear phase anisotropy of about 3.10^{-4} per pass. It will be clear from the above discussion that a cavity with a linear phase anisotropy should be assumed, rather than a linear absorption anisotropy, in order to explain the observed low-field polarization phenomena. In fact, however, the most likely situation will be a cavity with a relatively large linear phase anisotropy, and a relatively small linear absorption anisotropy.

D. Linear Phase and Absorption Anisotropy; a', $\phi' = 0$

Equation (79) reads

$$d\vartheta/dt = \frac{1}{2}a \sin 2(\vartheta - \vartheta_1) - \frac{1}{2}T\phi_0 \sin 2(\vartheta - \vartheta_2)$$
$$+ [\phi_0{}^2(S+1)/8(F-1)GS] \sin 4(\vartheta - \vartheta_2)$$
$$+ G(\mu_B g H_z/\hbar \gamma_D)M. \qquad (94)$$

The simultaneous presence of both kind of anisotropies gives rise to a more complicated behavior of the polarization plane. For instance, there is no abrupt flip, if at all, on tuning through line center at $H_z = 0$. Furthermore the flip is certainly different from $\frac{1}{2}\pi$ (if it is present). In general it occurs away from the line center.

In actual experiments a gradual change in polarization azimuth was indeed observed[4] on tuning through the line center. Furthermore the flip at zero field is not exactly 90°, but 5 to 10 deg smaller,[17] indicating that the main anisotropy present is a linear phase anisotropy, with a relatively small absorption anisotropy.

In principle, Eq. (94) can be used to determine precisely the cavity parameters a and ϕ_0 by analyzing the experiments. However, where the a values are estimated to be very small (about 10 to 100 times smaller than the ϕ_0 values) minor disturbances already change their actual value, making the polarization-flip phenomena nonreproducible.

ACKNOWLEDGMENTS

APPENDIX A

Apart from isotropic amplitude and phase changes, the transverse cavity field given by Eq. (2) is subject to anisotropic elements in the cavity. The isotropic losses and the anisotropies are very small (per interferometer pass). It is therefore possible to write the general loss tensor as the sum of suitably chosen infinitesimal tensors. We take for them tensors describing (1) an isotropic amplitude and phase loss, (2) a linear anisotropy in the amplitude, (3) a linear anisotropy in the phase, (4) a circular anisotropy in the amplitude, and (5) a circular anisotropy in the phase. The tensors are given in the representation adapted to left- and right-handed vectors as a basis. Each Γ can in a unique way be written as

$$\Gamma = \sum_{i=1}^{5} \Gamma_i, \qquad (A1)$$

where the five components are as follows:

$$\Gamma_1 = \epsilon_0 \begin{pmatrix} \Gamma & 0 \\ 0 & \Gamma \end{pmatrix}, \qquad (A2)$$

describing isotropic amplitude and phase loss (Γ is complex);

$$\Gamma_2 = \epsilon_0 \begin{pmatrix} 0 & a \exp(2i\vartheta_1) \\ a \exp(-2i\vartheta_1) & 0 \end{pmatrix}, \qquad (A3)$$

with a and ϑ_1 real, describing a linear anisotropy in the amplitude loss of magnitude $| a |$ —the main axes of this anisotropy are situated at $\vartheta = \vartheta_1$ and $\vartheta = \vartheta_1 + \frac{1}{2}\pi$;

$$\Gamma_3 = \epsilon_0 \begin{pmatrix} 0 & i\phi_0 \exp(2i\vartheta_2) \\ i\phi_0 \exp(-2i\vartheta_2) & 0 \end{pmatrix}, \qquad (A4)$$

with ϕ_0 and ϑ_2 real, describing a linear anisotropy in the phase loss of magnitude $| \phi_0 |$ —the main axes of this anisotropy are situated at $\vartheta = \vartheta_2$ and $\vartheta = \vartheta_2 + \frac{1}{2}\pi$;

$$\Gamma_4 = \epsilon_0 \begin{pmatrix} a' & 0 \\ 0 & -a' \end{pmatrix}, \qquad (A5)$$

with a' real, describing a circular anisotropy in the amplitude loss;

$$\Gamma_5 = \epsilon_0 \begin{pmatrix} i\phi' & 0 \\ 0 & -i\phi' \end{pmatrix}, \qquad (A6)$$

with ϕ' real, describing a circular anisotropy in the phase loss. The identification of the contributants (A3) to (A6) with pure absorption and phase anisotropies is no longer correct for large anisotropic elements. However, such cases are not considered.

APPENDIX B

The iteration procedure, applied to the density matrix equations (30)–(32), is as follows:

Suppose that the a_k level is excited at (z_0, t_0). The only nonvanishing zeroth-order density matrix element is then clearly

$$\rho_{a_k a_k}{}^{(0)}(t) = \exp[-\gamma_a(t-t_0)].\tag{B1}$$

In the first order in the **E** field we find the two nonvanishing matrix elements ($h=-1$ or $+1$):

$$\rho_{a_k b_{k+h}}{}^{(1)}(t) = i\int_{t_0}^{t} dt' V_{t'}(a_k, b_{k+h}) \exp[(-i(\omega_{a_k}-\omega_{b_{k+h}})-\gamma_{ab})(t-t')-\gamma_a(t'-t_0)],\tag{B2}$$

with their conjugates. In second order we have six nonvanishing matrix elements (and their conjugates):

$$\rho_{a_k a_k}{}^{(2)}; \; \rho_{a_k a_{k+2}}{}^{(2)}; \; \rho_{a_k a_{k-2}}{}^{(2)}; \; \rho_{b_{k+1} b_{k+1}}{}^{(2)}; \; \rho_{b_{k-1} b_{k-1}}{}^{(2)}; \; \rho_{b_{k+1} b_{k-1}}{}^{(2)}.$$

Substituting the appropriate indices m and m' they are given by

$$\rho_{a_m a_{m'}}{}^{(2)}(t) = -i\int_{t_0}^{t} dt' \sum_{h=\pm 1} [V_{t'}(a_m, b_{m+h}) \rho_{b_{m+h} a_{m'}}{}^{(1)}(t') - V_{t'}{}^*(a_m, b_{m'+h}) \rho_{a_m b_{m'+h}}{}^{(1)}(t')]$$

$$\times \exp[(-i(\omega_{a_m}-\omega_{a_{m'}})-\gamma_a)(t-t')], \quad\text{(B3)}$$

$$\rho_{b_m b_{m'}}{}^{(2)}(t) = -i\int_{t_0}^{t} dt' \sum_{h=\pm 1} [V_{t'}{}^*(a_{m+h}, b_m) \rho_{a_{m+h} b_{m'}}{}^{(1)}(t') - V_{t'}(a_{m'+h}, b_{m'}) \rho_{b_m a_{m'+h}}{}^{(1)}(t')]$$

$$\times \exp[(-i(\omega_{b_m}-\omega_{b_{m'}})-\gamma_b)(t-t')]. \quad\text{(B4)}$$

In third order there are eight nonvanishing matrix elements (and their conjugates), only four of them being relevant for the polarization vector (28):

$$\rho_{a_k b_{k+1}}{}^{(3)}; \; \rho_{a_k b_{k-1}}{}^{(3)}; \; \rho_{a_{k+2} b_{k+1}}{}^{(3)}; \; \rho_{a_{k-2} b_{k-1}}{}^{(3)}.$$

They are given by

$$\rho_{a_m b_{m'}}{}^{(3)}(t) = -i\int_{t_0}^{t} dt' \sum_{h=\pm 1} [V_{t'}(a_m, b_{m'+h}) \rho_{b_{m+h} b_{m'}}{}^{(2)}(t') - V_{t'}(a_{m'+h}, b_{m'}) \rho_{a_m a_{m'+h}}{}^{(2)}(t')]$$

$$\times \exp[(-i(\omega_{a_m}-\omega_{b_{m'}})-\gamma_{ab})(t-t')], \quad\text{(B5)}$$

where the appropriate indices m and m' have to be substituted. Introducing the function

$$C_{a_m b_{m'}}(a_k, v_z, z, t) \equiv \Lambda_a \int_{-\infty}^{t} dt_0 \rho_{a_m b_{m'}}(a_k, v_z, z-v_z(t-t_0), t_0, t) p_{m,m'},\tag{B6}$$

we can write the polarization vector (28) (confining ourselves for the moment to excitation in the a levels) as follows:

$$\mathbf{P}(z, t) = \tfrac{1}{2}\int_{-\infty}^{+\infty} dv_z \, W(v_z)$$

$$\times \sum_{k=-j_a}^{+j_a} [(C_{a_k b_{k+1}}{}^{(1)} + C_{a_k b_{k+1}}{}^{(3)} + C_{a_{k-2} b_{k-1}}{}^{(3)})(\mathbf{x}-i\mathbf{y}) + (C_{a_k b_{k-1}}{}^{(1)} + C_{a_k b_{k-1}}{}^{(3)} + C_{a_{k+2} b_{k+1}}{}^{(3)})(\mathbf{x}+i\mathbf{y})]+\text{c.c.,}\tag{B7}$$

where we wrote in abbreviated form $C(a_k, v_z, z, t) = C$. It can clearly be seen in (B7) that there are contributions from only two first-order and four third-order matrix elements. The calculation of the C functions is straightforward: The time integrations in (B2) and (B5) and the integration over t_0 are simple, as the time dependence of $E_\pm$ and $\phi_\pm$ in the perturbation matrix element V is ignored.[7] The first-order C functions are easily found to be

$$C_{a_k b_{k\pm 1}}{}^{(1)}(a_k, v_z, z, t) = (\Lambda_a/2\hbar\gamma_a) p_{k,k\pm 1}{}^2 \{E_\pm \exp[-i(\nu t+\phi_\pm)]\} \sin Kz \} D[Kv_z-f(k, k\pm 1)H_z],\tag{B8}$$

where

$$D[u] \equiv [u-(\omega-\nu)+i\gamma_{ab}]^{-1}\tag{B9}$$

and

$$f(l, l') \equiv (lg_a-l'g_b)\hbar^{-1}\mu_B.\tag{B10}$$

Expansion of the D function gives the desired specialization to polarization terms in zeroth and first order in the field:

$$D[Kv_z - f(k, k \pm 1) H_z] = D[Kv_z] + f(k, k \pm 1) H_z D^2[Kv_z] + \cdots. \tag{B11}$$

The approximation (B11) is justified for $| \mu_B g H_z / \gamma_{ab} \hbar | \ll 1$.

In the third-order C functions we leave out all terms that do not contribute either in the Doppler limit or in the local slope of the velocity distribution. The C functions are then given by

$$C_{a_k + a b_k + h}{}^{(3)} (a_k, v_z, z, t) = (-i\Lambda_a / 32\hbar^3 \gamma_a) \exp[-i(\nu t + \phi_{h-q})] \sin KzD[Kv_z - f(k, k+h) H_z]$$

$$\times \sum_{l, s = \pm 1} [E_l E_{-s} E_h \delta_{KR}(q + l + s) p_{k+q, k+h} p_{k+q, k+q+l} p_{k, k+q+l} p_{k, k+h}$$

$$\times \{ [\gamma_b + if(0, q + l - h) H_z]^{-1} (D[Kv_z - f(k, k+h) H_z] + D[-Kv_z - f(k, k+h) H_z])$$

$$+ ([\gamma_b + if(0, q + l - h) H_z]^{-1} + [\gamma_a + if(q, 0) H_z]^{-1})$$

$$\times (D[Kv_z + 2(\omega - \nu) + f(k, k + q + l) H_z] + D[-Kv_z + 2(\omega - \nu) + f(k, k + q + l) H_z]) \}$$

$$+ \sum_{m = \pm 1} E_l E_{-s} E_m \delta_{KR}(q) \delta_{KR}(l + s + m - h) p_{k+q, k+h} p_{k, k+l} p_{k+l+s, k+l} p_{k+l+s, k+h}$$

$$\times [\gamma_a + if(q - l - s, 0) H_z]^{-1} (D[Kv_z - f(k, k+l) H_z] + D[-Kv_z - f(k, k+l) H_z])], \tag{B12}$$

where we introduced the notations $E_{\pm 1} = E_\pm$ and $\phi_{\pm 1} = \phi_\pm$. By expanding all denominators in (B12) we easily obtain the zeroth- and first-order contribution in H_z. Retaining only terms in first order in H_z is justified for

$$| \mu_B g H_z / \hbar | \ll \gamma_a, \gamma_b \tag{B13}$$

implying field splittings $\lesssim 1$ Mc/sec.

APPENDIX C

In calculating the polarization vector (28), or alternatively (B7), a number of velocity integrations have to be performed. The $\mathbf{P}^{(1)}$ vector contains the integral

$$\int_{-\infty}^{+\infty} dv \, W(v) \{ D[Kv] + f(k, k \pm 1) H_z D^2[Kv] \}. \tag{C1}$$

We find

$$\mathrm{Im} \int_{-\infty}^{+\infty} dv \, W(v) D[Kv] = (\pi/K) W[(\omega - \nu)/K] + \cdots, \tag{C2}$$

in the Doppler limit, i.e., neglecting terms that are an order γ_{ab}/γ_D smaller. This integral contributes to the phenomenological constant α (i.e., to the first-order absorptive part of $\mathbf{P}$).

For the constant σ (first-order dispersive part of $\mathbf{P}$) we need

$$\mathrm{Re} \int_{-\infty}^{+\infty} dv \, W(v) D[Kv] = K^{-1} \int_{-\infty}^{+\infty} dv' \frac{\nu' W[(\omega - \nu + \nu')/K]}{(\nu'^2 + \gamma_{ab}^2)}, \tag{C3}$$

largely depending on the full shape of $W(v)$. However, σ does not enter in our equations of motion (13), (14), and (15). We therefore do not calculate (C3). It can be found in Ref. 13.

The constant α' (or the absorptive part of $\mathbf{P}$, linear in $\mathbf{E}$ and $\mathbf{H}$) is proportional to

$$\mathrm{Im} \int_{-\infty}^{+\infty} dv \, W(v) D^2[Kv] = -(\pi/K^2)(dW/dv)_{v=(\omega - \nu)/K} + \cdots \tag{C4}$$

and is almost proportional to the local slope in the Doppler profile. The constant σ' (or the dispersive part of $\mathbf{P}$, linear in $\mathbf{E}$ and $\mathbf{H}$) is proportional to

$$\mathrm{Re} \int_{-\infty}^{+\infty} dv \, W(v) D^2[Kv] = K^{-1} \int_{-\infty}^{+\infty} dv' \frac{(\nu'^2 - \gamma_{ab}^2) W[(\omega - \nu + \nu')/K]}{(\nu'^2 + \gamma_{ab}^2)^2}, \tag{C5}$$

largely depending on the full shape of the Doppler profile. The related integral $J(s, r)$ [see Eq. (49)] is plotted in Fig. 1, where a Maxwellian distribution is taken for $W(v)$.

The velocity integrations in the case of the $\mathbf{P}^{(3)}$ vector are as follows. Taking first $H_z=0$, two types of integrals survive in the Doppler limit. The first type is

$$I_1=\int_{-\infty}^{+\infty}dv\ W(v)D[Kv]D[-Kv+2(\omega-\nu)]=-(\pi/K\gamma_{ab})W[(\omega-\nu)/K]+\cdots,\qquad(C6)$$

giving the main contributions to the constants β_1 and β_2, i.e., to the third-order absorptive part of $\mathbf{P}$. The second type of integral is

$$I_2=\int_{-\infty}^{+\infty}dv\ W(v)D[Kv]D[-Kv]=(\pi/K)[-\gamma_{ab}+i(\omega-\nu)]\mathcal{L}(\omega-\nu)W[(\omega-\nu)/K]+\cdots.\qquad(C7)$$

Re I_2 contributes to the β coefficients; Im I_2 to the ρ coefficients. They represent the well-known hole–hole interaction contribution. Contributions proportional to the local slope of $W(v)$ arise mainly from

$$I_3=\int_{-\infty}^{+\infty}dv\ W(v)D^2[Kv]=-(\pi i/K^2)\ (dW/dv)_{v=(\omega-\nu)/K}+\cdots\qquad(C8)$$

and are of a dispersive nature. A comparison of I_3 with Im I_2 shows that the former is relevant to frequencies not too close to line center. For $|\omega-\nu|=5\gamma_{ab}$ the contribution from I_3 is already 20% of that of Im I_2. In the case of a travelling wave maser, where the hole–hole interaction is absent, the main nonlinear dispersive effect comes from I_3. The integral I_1 has no contribution proportional to the slope of $W(v)$; the integral I_2 has. However, this contribution cannot be calculated separately. It has to be combined with the contribution of

$$I_4=\int_{-\infty}^{+\infty}dv\ W(v)D[Kv]D[Kv+2(\omega-\nu)].\qquad(C9)$$

We find

$$I_2+I_4=(\pi/K)[-\gamma_{ab}+i(\omega-\nu)]\mathcal{L}(\omega-\nu)\{W[(\omega-\nu)/K]+(\gamma_{ab}/K)\ (dW/dv)_{v=(\omega-\nu)/K}\}+\cdots.\qquad(C10)$$

We ignore the slope term in (C10). Its real part is small compared to Re I_1. Its imaginary part is small compared to Im I_3, except for operation near line center where Im I_3 is small compared to Im I_2.

Taking $H_z\neq0$, we meet the new types of integrals (all are calculated in the Doppler limit)

$$I_5=\int_{-\infty}^{+\infty}dv\ W(v)D^2[Kv]D[-Kv]=\int_{-\infty}^{+\infty}dv\ W(v)D[Kv]D^2[-Kv]$$

$$=(\pi/K)W[(\omega-\nu)/K]\mathcal{L}^2(\omega-\nu)\{\gamma_{ab}(\omega-\nu)-i\tfrac{1}{2}[(\omega-\nu)^2-\gamma_{ab}^2]\}+\cdots,\qquad(C11)$$

$$I_6=\int_{-\infty}^{+\infty}dv\ W(v)D^2[Kv]D[-Kv+2(\omega-\nu)]$$

$$=\int_{-\infty}^{+\infty}dv\ W(v)D[Kv]D^2[-Kv+2(\omega-\nu)]=i(\pi/2H\gamma_{ab}^2)W[(\omega-\nu)/K]+\cdots.\qquad(C12)$$

Substituting the C functions (B8) and (B12) in (B7) and substituting the integrals calculated above, the final expression for $\mathbf{P}$ is obtained in a straightforward way. The result of this substitution is found in Eqs. (36)–(47), where the coefficients from Eqs. (7) and (8) are given, which, according to Eq. (3) is equivalent to giving $\mathbf{P}$.